Chelation of diamine ligands to zinc porphyrin monolayers amide-linked to glass

Duncan W. J. McCallien, Paul L. Burn* and Harry L. Anderson*

Dyson Perrins Laboratory, University of Oxford, South Parks Road, Oxford, UK OX1 3QY

A pentafluorophenol active-ester porphyrin has been synthesised and covalently attached to an aminopropylsilylated glass surface by amide bond formation. Zinc is inserted into the surface-bound porphyrins and their interaction with amine ligands is investigated by UV–VIS spectroscopy. The high affinity of the zinc porphyrin monolayers for bidentate ligands such as 1,4-diazabicyclo[2.2.2]octane, 4,4′-bipyridyl and 1,3-di(4-pyridyl)propane demonstrates that the porphyrins are in close proximity on the surface and yet are not so tightly packed as to prevent ligand intercalation. Effective molarities of up to 0.35 mol dm^{-3} are observed.

Introduction

Porphyrins have been widely used in photovoltaic devices because they support efficient photoinduced charge separation.[1] Porphyrin thin films can be prepared by electropolymerisation,[2] solution[3] or melt[4] casting and vacuum deposition.[5] These approaches give layers whose thickness is difficult to govern. Deposition of Langmuir–Blodgett films allows control of the thickness and the orientation of the porphyrins on the surface.[6] Porphyrin monolayers have also been prepared by using gold–thiol chemistry[7] and other types of covalent[8] and non-covalent interactions.[9]

As part of our work on photovoltaic devices we have explored amide coupling as a way of linking porphyrins to a glass surface. We sought to discover how far apart the chromophores are and how much they are able to move when anchored to the surface. The average surface density can be estimated from the UV–VIS absorption, but this does not tell us how far apart the chromophores are because we cannot assume that the surface layer is perfectly flat, nor that the coverage is uniform. The affinity of covalent metalloporphyrin oligomers for multidentate ligands has been found to be a sensitive probe for the preferred porphyrin–porphyrin distance and flexibility in these molecules in solution.[10] We have applied the same technique to metalloporphyrins covalently linked to a surface. Here we report that our solid phase porphyrin monolayers have a high affinity for linear bidentate ligands, just like covalent porphyrin oligomers in solution. We show that measuring the ligand-affinity of a porphyrin monolayer is a way of probing its surface structure. Binding to bidentate ligands may also be a way of increasing the order at the surface, by forming two-dimensional crystalline networks or by the template-directed positioning of surface functionality. Ligand coordination is potentially a way of binding photoactive components to a porphyrin-covered surface. The quantitative understanding of chelation to surface functional groups is also relevant to the biological recognition of cell membranes and viruses.[11]

Porphyrin monolayers on silica have previously been used as chromatographic stationary phases for separating anions. Sapphyrins amide-linked to silica have a high selective affinity for phosphate and arsenate anions[12] whilst cobalt(III), manganese(III) and indium(III) porphyrins bind nitrite and chloride ions.[2b,8c] Porphyrin functionalised solid supports can also bind polycyclic aromatic hydrocarbons[8d] and have been used to separate fullerenes.[8e] Porphyrins on glass have been used as pH sensors[2c] and as chemical sensors.[6c]

* E-Mail: harry.anderson@dyson.ox.ac.uk and plburn@vax.ox.ac.uk

Results and discussion

Solution phase synthesis

We aimed to prepare an active ester porphyrin which could be coupled efficiently to an aminopropylsilylated glass. We designed the pentafluorophenol ester **1** with *n*-butyl β-

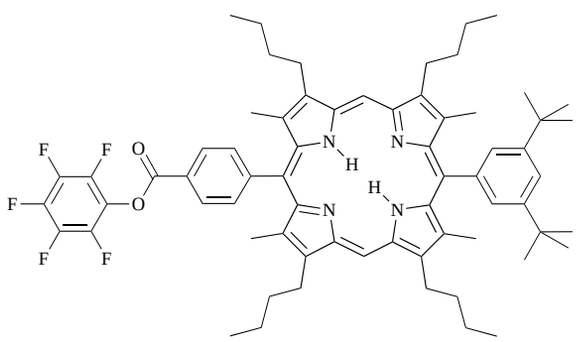

1

substituents and *tert*-butyl aryl substituents to impart high solubility and to give a high yielding porphyrin synthesis. Trifluoroacetic acid catalysed condensation of a 1:1 mixture of aldehydes **2** and **3** with dipyrromethane **4** followed by oxidation with 2,3-dichloro-5,6-dicyano-1,4-benzoquinone (DDQ) gave porphyrins **5**, **6** and **7** (Scheme 1).[13] These were readily separated by column chromatography on silica and isolated in 17, 42 and 17% yields respectively. Porphyrin **6** was hydrogenolysed to the carboxylic acid **8** in 80% yield and then coupled to pentafluorophenol using dicyclohexylcarbodiimide (DCC) and 4-pyrrolidinopyridine (POP) to give **1** in 66% yield. We also converted **8** into the acid chloride **9** using oxalyl chloride and thence to the zinc complex of the propylamide, **Zn-10**, using propylamine, with catalytic 4-dimethylaminopyridine, followed by addition of zinc acetate. Isolation of **10** was necessary because **Zn-10** was difficult to separate from propylamine hydrochloride. The porphyrin amide **10** and its zinc complex **Zn-10** were used as model compounds for comparison with the surface linked porphyrins.

Surface functionalisation and solid phase synthesis

Zinc porphyrin functionalised glass surfaces, which we designate **Glass·Zn-11**, were prepared as shown in Scheme 2. Glass microscope slides were aminopropylsilylated by treatment with 3-aminopropyltriethoxysilane in toluene at 100 °C for 5 h.[14] Porphyrins were then covalently attached to the surface using a solution of **1** in toluene to give **Glass·H_2-11**; absorption spec-

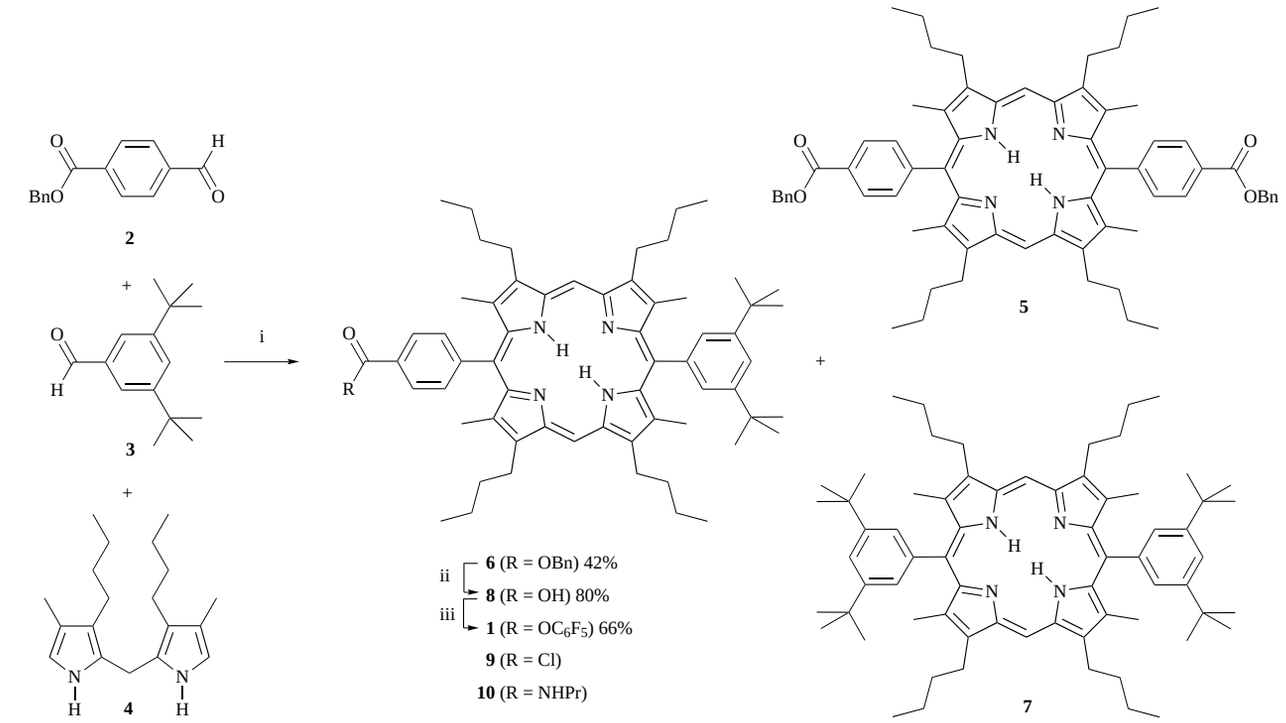

Scheme 1 *Reagents and conditions:* i, (a) F_3CCO_2H, CH_2Cl_2; (b) DDQ; ii, 10% Pd–C, H_2, CH_2Cl_2; iii, DCC, F_5C_6OH, POP

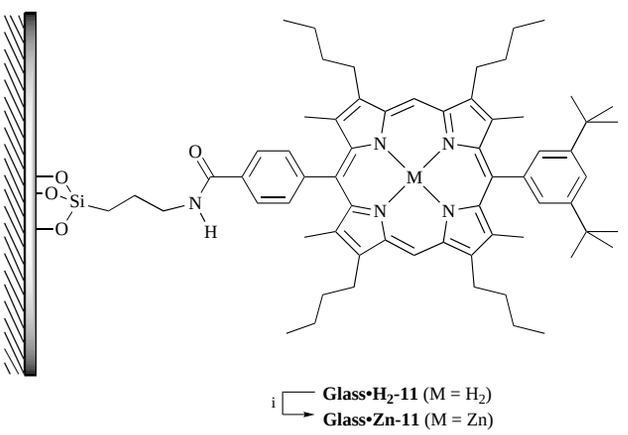

Scheme 2 *Reagents and conditions:* i, $Zn(OAc)_2 \cdot 2H_2O$, $CHCl_3$

troscopy showed that the reaction reached completion after 1 h at 100 °C. Some porphyrin was found to physisorb onto the surface[8b] and this was removed by washing with 1% trifluoroacetic acid in dichloromethane. The surface bound porphyrins were metallated with zinc by refluxing with zinc acetate in chloroform; absorption spectroscopy showed that the reaction reached completion after 5 min. Some porphyrin was lost from the surface during metallation. The integrated extinction coefficient discussed below show that this loss corresponds to about 10% of the chromophores.

We also tried reacting the porphyrin acid chloride **9** with aminopropylsilylated glass, but this reaction gave less reproducible results than the pentafluorophenol ester **1**, which is probably a result of the fact that **1** is a stable crystalline solid whereas **9** is too reactive to be isolated. Porphyrin **9** needs to be generated in solution immediately before use and tends to undergo side reactions during coupling to amines.

UV–VIS spectra of porphyrin monolayers

The absorption spectrum of dry **Glass·H_2-11** in air is compared with that of **10** in dichloromethane solution in Fig. 1(*a*). The absorption bands of the surface bound porphyrin are broader than those in solution and the Soret band is red shifted by 7 nm. This broadening and red-shifting can be attributed to exciton

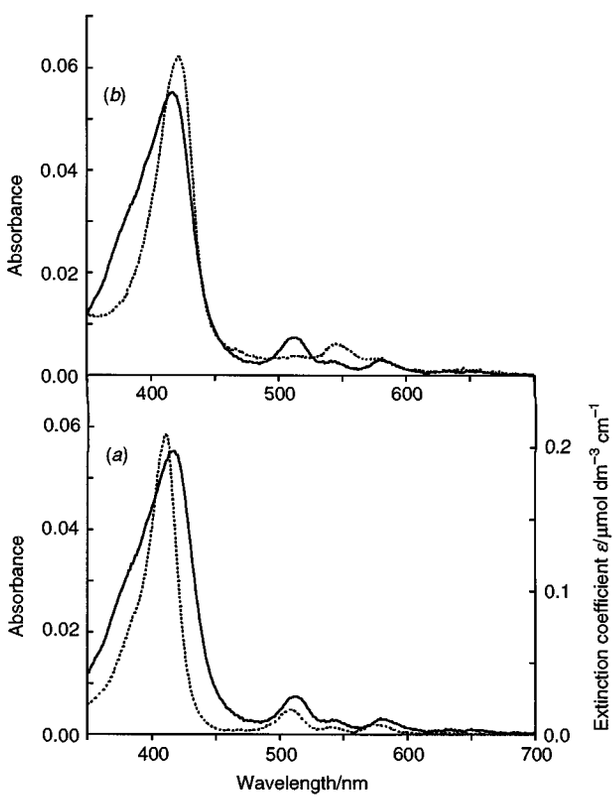

Fig. 1 Absorption spectra of porphyrin monolayers. (*a*) Comparison of **Glass·H_2-11** absorbance in air (continuous line) with the free base porphyrin **10** extinction coefficient in dichloromethane (dashed line). (*b*) Comparison of **Glass·H_2-11** absorbance (continuous line) with the same sample after metallation, **Glass·Zn-11** (dashed line) both in air.

coupling between porphyrins in close proximity on the surface. The spectra of **Glass·H_2-11** and **Glass·Zn-11** are compared in Fig. 1(*b*); the change in the shape of the Q-band shows that the porphyrins have been metallated.

The average surface density of chromophores ρ (mol cm^{-2}) was estimated by integrating the Soret abosorption bands of **Glass·H_2-11** and **Glass·Zn-11**, plotted on an energy scale, and

comparing these areas with those of the extinction coefficient spectra of **10** and **Zn-10** in solution. This procedure assumes that the integrated extinction coefficient (and oscillator strength †) of each porphyrin on the surface is the same as that of a porphyrin in solution, which is better than simply comparing peak absorptions, because the spectra of surface porphyrins are broader than solution spectra. According to the Beer–Lambert law [eqn. (1)], where $\int \varepsilon \, d\nu$ is the integrated extinction

$$\int \varepsilon \, d\nu = \frac{\int A \, d\nu}{cl} = \frac{1}{1000} \times \frac{\int A \, d\nu}{\rho} \qquad (1)$$

coefficient (mol^{-1} dm^3 cm^{-1} integrated with respect to the frequency ν in cm^{-1}), $\int A \, d\nu$ is the integrated absorption, c is concentration (mol dm^{-3}) and l is the path length (cm). So the surface density of chromophores is given by eqn. (2).

$$\rho = \frac{1}{1000} \times \frac{\int A_{\text{on glass}} \, d\nu}{\int \varepsilon_{\text{in solution}} \, d\nu} \qquad (2)$$

The Soret bands of **Glass·H_2-11** and **Glass·Zn-11** had peak absorptions of 0.055 and 0.062 and integrated absorption coefficients of 66 and 65 cm^{-1} respectively (per surface, with the surface larger than the spectrometer window). The Soret bands of **10** and **Zn-10** have integrated extinction coefficient of 3.8×10^8 and 4.5×10^8 mol^{-1} dm^3 cm^{-2} respectively. So the surface density of chromophores ρ for **Glass·H_2-11** and **Glass·Zn-11** is 1.7×10^{-10} and 1.5×10^{-10} mol cm^{-2}, which corresponds to an area per molecule of 98 and 110 $Å^2$ respectively. Molecular mechanics calculations show that the porphyrin has a cross-section area of *ca.* 160 $Å^2$ if it stands perpendicular to the surface, or *ca.* 340 $Å^2$ if it lies flat on the surface. So allowing for experimental error, the surface density of chromophores is the same as the expected value for porphyrins stacked on edge on a perfectly flat surface. In fact the surface is unlikely to be perfectly flat. Surface profile measurements, and a preliminary AFM investigation,‡ on clean silylated glass microscope slides show a deviation from planarity of around ±350 Å, whereas uncoated slides are flat to within ±150 Å.[15]

Binding studies

The affinity of **Glass·Zn-11** for amine ligands was measured by recording the absorption spectrum of the porphyrin covered surface immersed in dichloromethane containing the ligand at a range of concentrations. On addition of amines a red shift was observed in the Soret band, which is similar to that seen when zinc porphyrins bind amines in solution. The binding data, for both monodentate and bidentate ligands, were found to fit well to calculated curves for 1:1 binding with a single binding constant (the Langmuir isotherm). The binding constants of **Glass·Zn-11** are compared in Table 1 with those of **Zn-10** in dichloromethane. This model compound was chosen because it should have an identical intrinsic ligand-affinity to the surface bound porphyrin, since the electronic effect of a propyl amide group should be the same as that of the silylpropyl amide linker (the ligand affinities of zinc porphyrins are sensitive to electronic effects).[16] Five ligands were used in this study: pyridine (Py), quinuclidine (Quin), 1,4-diazabicyclo[2.2.2]octane (DABCO), 4,4′-bipyridyl (Bipy) and 1,3-di(4-pyridyl)propane (Py_2pr). These bidentate ligands were selected to cover a range of nitrogen–nitrogen distances; the monodentate ligands were chosen to have similar intrinsic zinc affinities to their bidentate analogues. All binding constants were measured at least twice and errors were typically ±10% for **Zn-10** and ±20% for **Glass·Zn-11**.

Table 1 Binding constants from UV–VIS titrations

Ligand	K(**Zn-10**)/ mol^{-1} dm^3	K(**Glass·Zn-11**)/ mol^{-1} dm^3	Span/Å	EM/mol dm^{-3}
Py	1.8×10^3	0.74×10^3	—	—
Quin	83×10^3	50×10^3	—	—
Bipy	2.4×10^3	84×10^3	12.1	0.35
Py_2pr	5.3×10^3	370×10^3	14.5	0.31
DABCO	140×10^3	$24\,000 \times 10^3$	7.6	0.013

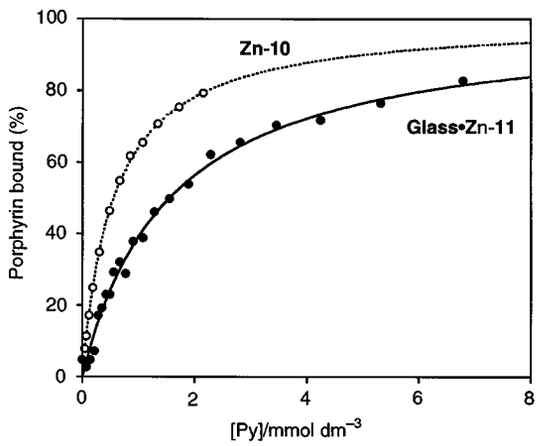

Fig. 2 Isotherm for binding pyridine (Py) to the porphyrin monolayer **Glass·Zn-11** (●) compared with that for the porphyrin in solution **Zn-10** (○)

We found that monodentate ligands, pyridine and quinuclidine, bind more strongly to the porphyrin in solution, **Zn-10**, than to that on the surface **Glass·Zn-11**. This is illustrated for pyridine in Fig. 2. It is not surprising that the binding sites are less accessible at the surface, as some steric hindrance is to be expected. A more polar environment at the surface could also cause weaker binding. However it is remarkable that the binding constants for **Glass·Zn-11** are only reduced by a factor of 2–3; the surface porphyrins are almost as accessible as porphyrins in solution. We excluded the possibility that the weaker binding of **Glass·Zn-11** could be due to any free amine groups on the surface competing for coordination sites, by acetylating **Glass·Zn-11** with acetyl chloride; this had no effect on the affinity of the surface for pyridine.

All the bidentate ligands bind more strongly to **Glass·Zn-11** than to **Zn-10** as exemplified by the binding curves for Bipy in Fig. 3. This demonstrates that all these ligands are able to intercalate into the porphyrin monolayer and reach between pairs of zinc centres (Scheme 3). The degree of chelation can be quantified by the effective molarity EM. In general the effective molarity of a bidentate ligand for a multi-site receptor is defined as in eqn. (3), where $K_{\text{bidentate}}$ is the chelation enhanced binding

$$EM = \frac{K_{\text{bidentate}}}{(K_{\text{monodentate}})^2} \qquad (3)$$

constant of the bidentate ligand and $K_{\text{monodentate}}$ is the binding constant of one end of the bidentate ligand. $K_{\text{monodentate}}$ cannot normally be measured, so it is approximated to the binding constant of the bidentate ligand for a single site receptor, corrected by the statistical factor of 2 and by the relative affinity of the multi-site receptor for monodentate ligands.[10a] Thus we have calculated EM using eqn. (4).

† The oscillator strength f is defined as:

$$f = \frac{4.319 \times 10^{-9}}{n} \int \varepsilon \, d\nu$$

where n is the refractive index (1.42 for CH_2Cl_2), ε is the extinction coefficient (mol^{-1} dm^3 cm^{-1}) and ν is the frequency in wavenumbers (cm^{-1}). The Soret bands of **10** and **Zn-10** have oscillator strengths of 1.2 and 1.4, respectively.

‡ We are grateful to Dr B. A. Coles for carrying out a preliminary AFM examination of silylated glass surfaces.

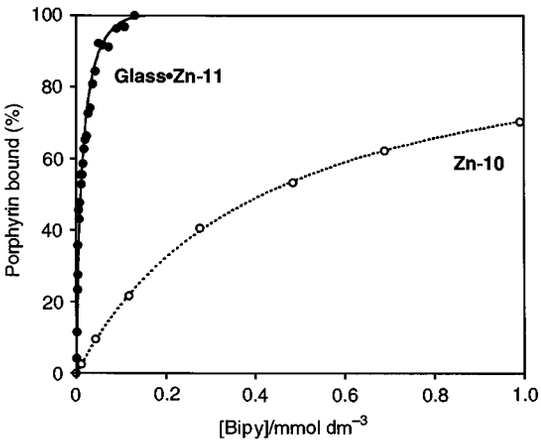

Fig. 3 Isotherm for binding 4,4′-bipyridyl (Bipy) to the porphyrin monolayer **Glass·Zn-11** (●) compared with that for the porphyrin in solution **Zn-10** (○)

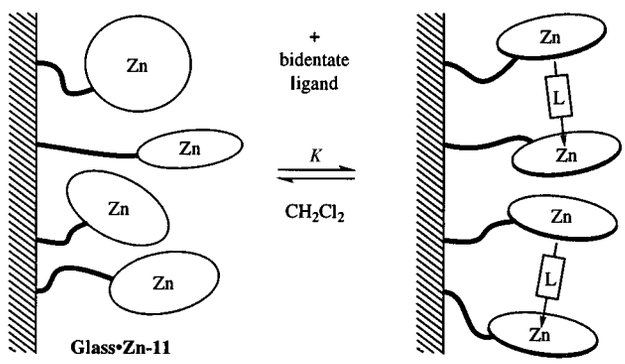

Scheme 3

$$EM = \frac{K_{\text{bidentate on glass}}}{\left(\frac{K_{\text{bidentate in soln}}}{2} \times \frac{K_{\text{monodentate on glass}}}{K_{\text{monodentate in soln}}}\right)^2} \qquad (4)$$

The effective molarities for the bidentate ligands binding to **Glass·Zn-11** are listed in Table 1 together with their spans. We define the span of a bidentate ligand as its optimal zinc porphyrin centre–centre distance. These were estimated from crystallographic data for Bipy[17] and DABCO[18] and from the MM2 minimised structure for Py_2pr.

Bipy and Py_2pr both give effective molarities of about 0.3 mol dm^{-3}, whereas DABCO gives an *EM* of only around 0.01 mol dm^{-3}. This implies that the porphyrins can easily get into positions where they are 12–15 Å apart, but that geometries where they are only 7.6 Å apart are less favourable. The strongest binding is observed for DABCO because of the high microscopic binding constant for one end of a DABCO ligand. The end point of the DABCO–**Glass·Zn-11** titration can be determined by simulation analysis of the binding isotherm and used to estimate the number of binding sites on the surface. A sample of **Glass·Zn-11** with a functionalised surface area of 3.0 cm^2 gave a best fit end point after *ca.* 3×10^{-10} moles of DABCO had been added. As each DABCO molecule binds to two zinc centres this corresponds to a surface density of chromophores ρ of 2×10^{-10} mol cm^{-2}, which compares well with the value obtained from the integrated absorption (1.5×10^{-10} mol cm^{-2}).

Conclusions

We have shown that amide-linked zinc porphyrin monolayers can be prepared which bind monodentate amines almost as well as zinc porphyrins in free solution. The binding sites are pre-organised on the surface, so these monolayers have a high affinity for bidentate ligands. The surface-bound porphyrins are flexible enough to chelate to bidentate ligands with spans in the range 7.6–14.5 Å. They chelate more efficiently to the longer ligands, Bipy and Py_2pr ($EM = 0.3$ mol dm^{-3}), than to the shorter ligand DABCO ($EM = 0.01$ mol dm^{-3}). We believe this is the first time that chelation to surface binding sites has been measured and quantified in terms of effective molarities.

Experimental

Glass microscope slides (soda glass) were obtained from BDH (as cut, 26 × 76 mm, 0.8–1.0 mm) and cleaned to remove grease by sonication in a Sonicor apparatus for 15 min, firstly in 1:1 v/v acetone–distilled water, then in isopropyl alcohol and finally in dichloromethane. Solvents such as toluene and dichloromethane were distilled over calcium hydride prior to use. Light petroleum refers to the bp 60–80 °C fraction.

UV measurements were carried out on a Perkin-Elmer Lambda 14P spectrophotometer at 22 °C in dichloromethane. ^{1}H, ^{19}F and ^{13}C NMR spectra were run on Bruker AM-200, 250 or 500 MHz instruments using deacidified deuteriochloroform; coupling constants *J* are quoted in Hz. FAB mass spectra were obtained on a VG Autospec instrument from a *m*-nitrobenzyl alcohol matrix in Oxford or by the EPSRC service at Swansea. IR spectra were recorded in KBr discs or dichloromethane using a Perkin-Elmer Paragon 1000 spectrophotometer. Surface profiling of glass slides, cleaned by sonication in dichloromethane, was done with a 'Dektak^3' surface profiler instrument. TLC data is quoted for silica based slides.

p-Formylbenzoic acid phenylmethyl ester 2[19]

Dicyclohexylcarbodiimide (4.12 g, 0.02 mol) in dry dichloromethane (20 cm^3) was added dropwise to a stirred solution of *p*-formylbenzoic acid (3.0 g, 0.02 mol), benzyl alcohol (2.16 g, 0.02 mol) and pyrrolidinopyridine (2.96 g, 0.02 mol) at 0 °C in dry dichloromethane (20 cm^3). It was stirred overnight during which time it warmed up to room temperature. The dicyclohexylurea was then filtered off from the yellow solution and the latter was evaporated to dryness. Purification by column chromatography on flash silica eluting with 17:3 v/v light petroleum–ethyl acetate yielded **2** (4.55 g, 95%); $\nu_{max}(CH_2Cl_2)$/cm^{-1} 2825, 1722, 1705, 1605, 1580 and 1500; δ_H(200 MHz) 5.38 (2H, s), 7.40 (5H, m), 7.92 (2H, d, *J* 8.1), 8.21 (2H, d, *J* 8.2) and 10.08 (1H, s); δ_C(125 MHz) 67.26, 128.29, 128.45, 128.64, 129.46, 130.25, 135.04, 135.50, 139.17, 165.34 and 191.55; *m/z* (CI) 258 (M + NH_4^+).

4-[2,8,12,18-Tetrabutyl-3,7,13,17-tetramethyl-15-(3,5-di-*tert*-butylphenyl)-21*H*,23*H*-porphyrin-5-yl]benzoic acid phenylmethyl ester 6

2,8-Dimethyl-3,7-dibutyl-5,10-dihydrodipyrromethane[13] **4** (1.488 g, 5.24 mmol), benzyl *p*-formylbenzoate **2** (0.629 g, 2.62 mmol) and 3,5-di-*tert*-butylbenzaldehyde[20] **3** (0.571 g, 2.62 mmol) were added to dry dichloromethane (170 cm^3) and thoroughly saturated with nitrogen. Trifluoroacetic acid (68 μl, final reaction concentration 5 mmol dm^{-3}) was added and the mixture stirred for 2 h, initially at 0 °C and then at room temperature under nitrogen. DDQ (1.78 g, 7.86 mmol) was added under air, stirred for 10 min and then saturated aqueous sodium hydrogen carbonate (75 cm^3) was added. After washing with water (3 × 200 cm^3), the organic layer was evaporated to dryness and the three porphyrins separated by flash chromatography. The reaction mixture was applied to a flash silica column of 23 × 4.5 cm in the minimum volume of dichloromethane. The most mobile 5,15-(3,5-di-*tert*-butylphenyl)-2,8,12,18-tetrabutyl-3,7,13,17-tetramethyl-21*H*,23*H*-porphyrin **7** eluted first (0.437 g, 17%) from the column in a solvent mix-

ture of 7:3 v/v light petroleum–dichloromethane; R_F(1:3 CH_2Cl_2–light petroleum) 0.41; λ_{max}/nm (log ε/dm^3 mol^{-1} cm^{-1}) 410 (5.43), 508 (4.34), 541 (3.90), 575 (4.00) and 627 (3.70); δ_H(200 MHz) −2.40 (2H, br s), 1.10 (12H, t, *J* 7.3), 1.50 (36H, s), 1.78 (8H, sextet, *J* 7.4), 2.17 (8H, qn, *J* 7.4), 2.45 (12H, s), 3.99 (8H, t, *J* 7.6), 7.80 (2H, t, *J* 1.7), 7.91 (4H, d, *J* 1.8) and 10.22 (2H, s); δ_C(125 MHz) 14.74, 23.91, 27.06, 32.18, 35.65, 36.00, 97.28, 119.65, 121.55, 128.13, 136.94, 141.54, 141.82, 143.48, 145.65 and 150.33; *m/z* (+ve FAB) 966.7 (M^+). The second fraction was eluted with 1:1 light petroleum–dichloromethane and subsequently recrystallised from hot light petroleum yielding **6** (1.088 g, 42%); R_F(1:3 CH_2Cl_2–light petroleum) 0.24; λ_{max}/nm (log ε/dm^3 mol^{-1} cm^{-1}) 410 (5.48), 508 (4.43), 542 (3.95), 575 (4.08) and 627 (3.00); ν_{max}(KBr)/cm^{-1} 1720 (C=O); δ_H(500 MHz) −2.29 (2H, s), 1.18 (6H, t, *J* 7.4), 1.20 (6H, t, *J* 7.4), 1.60 (18H, s), 1.84 (8H, sextet, *J* 7.3), 2.25 (8H, m), 2.55 (6H, s), 2.56 (6H, s), 4.08 (8H, t, *J* 7.9), 5.65 (2H, s), 7.49 (1H, t, *J* 7.5), 7.56 (2H, t, *J* 7.6), 7.70 (2H, d, *J* 7.3), 7.91 (1H, t, *J* 1.8), 8.01 (2H, d, *J* 1.8), 8.28 (2H, d, *J* 8.0), 8.56 (2H, d, *J* 8.0) and 10.33 (2H, s); δ_C(125 MHz) 14.24, 14.93, 23.31, 23.41, 26.49, 26.54, 31.69, 35.18, 35.50, 67.11, 97.06, 116.17, 119.74, 121.18, 127.56, 128.44, 128.50, 128.75, 128.89, 129.97, 133.26, 135.60, 136.09, 136.74, 140.89, 141.37, 141.54, 143.18, 143.50, 144.42, 145.35, 147.79, 149.94 and 166.78; *m/z* (+ve FAB) 989.9 (M^+). The third fraction was eluted from the column using dichloromethane yielding 4,4′-(2,8,12,18-tetrabutyl-3,7,13,17-tetramethyl-21*H*,23*H*-porphyrin-5,15-diyl)dibenzoic acid bis(phenylmethyl) ester **5** (0.458 g, 17%); R_F(1:3 CH_2Cl_2–light petroleum) 0.10; λ_{max}/nm (log ε/dm^3 mol^{-1} cm^{-1}) 410 (5.39), 508 (4.40), 541 (3.90), 576 (4.00) and 626 (3.48); δ_H(200 MHz) −2.42 (2H, s), 1.08 (12H, t, *J* 7.3), 1.71 (8H, sextet, *J* 7.4), 2.15 (8H, qn, *J* 7.4), 2.45 (12H, s), 3.97 (8H, t, *J* 7.5), 5.57 (4H, s), 7.48 (6H, m), 7.63 (4H, dd, *J* 7.8 and 1.5), 8.17 (4H, d, *J* 8.1), 8.46 (4H, d, *J* 8.1) and 10.24 (2H, s); δ_C(125 MHz) 14.21, 14.89, 23.28, 26.43, 35.46, 67.10, 97.25, 116.69, 128.43, 128.49, 128.73, 128.91, 130.02, 133.13, 135.84, 136.04, 141.52, 143.63, 144.54, 147.52 and 166.71; *m/z* (+ve FAB) 1011.4 (M^+).

4-[2,8,12,18-Tetrabutyl-3,7,13,17-tetramethyl-15-(3,5-di-*tert*-butylphenyl)-21*H*,23*H*-porphyrin-5-yl]benzoic acid 8

Palladium (10%) on charcoal (200 mg) was added to a solution of **6** (0.800 g, 8.09 × 10^{-4} mol) in dry dichloromethane (100 cm^3) and the mixture degassed using the water aspirator. It was then stirred rapidly under an atmosphere of hydrogen gas for 3.5 h and monitored by TLC. The palladium on charcoal was removed by filtration through Celite and the solvent removed under reduced pressure. After redissolving in dichloromethane, the product was separated from the remaining starting material using a short flash column (10 × 3 cm) eluting initially with 1% methanol in dichloromethane to remove the reactant and then with 2% methanol to yield **8** (584 mg, 80%); R_F-($CHCl_3$) 0.04; λ_{max}/nm (log ε/dm^3 mol^{-1} cm^{-1}) 410 (5.43), 508 (4.34), 541 (3.90), 575 (4.00) and 627 (3.70); ν_{max}(KBr)/cm^{-1} 1691 (C=O); δ_H(500 MHz) 1.16 (6H, t, *J* 7.1), 1.17 (6H, t, *J* 7.1), 1.56 (18H, s), 1.81 (8H, m, *J* 7.7), 2.24 (8H, quintet, *J* 7.7), 2.52 (6H, s), 2.56 (6H, s), 4.05 (8H, br t), 7.87 (1H, s), 7.98 (2H, s), 8.32 (2H, d, *J* 7.7), 8.60 (2H, d, *J* 7.6) and 10.31 (2H, s); δ_C(125 MHz) 14.25, 14.94, 23.33, 23.40, 26.52, 31.68, 35.16, 35.50, 97.10, 116.01, 119.80, 121.19, 127.55, 129.16, 129.40, 133.44, 135.52, 136.76, 140.86, 141.39, 141.56, 143.19, 143.58, 144.35, 145.36, 148.66, 149.96 and 171.93; *m/z* (+ve FAB) 899.6 (M^+).

4-[2,8,12,18-Tetrabutyl-3,7,13,17-tetramethyl-15-(3,5-di-*tert*-butylphenyl)-21*H*,23*H*-porphyrin-5-yl]benzoic acid 2,3,4,5,6-pentafluorophenyl ester 1

Dicyclohexylcarbodiimide (DCC) (21 mg, 0.1 mmol) in dry dichloromethane (20 cm^3) was added dropwise to a solution of **8** (100 mg, 0.1 mmol), pentafluorophenol (22 mg, 1.2 mmol) and 4-pyrrolidinopyridine (POP) (15 mg, 0.1 mmol) in dry dichloromethane (25 cm^3) at 0 °C. The mixture was stirred for 5 h and simultaneously allowed to warm to room temperature. The urea was removed by filtration and the solvent removed under reduced pressure. The products were purified by flash column chromatography eluting with chloroform on 15 × 3 cm silica. The product was the first band to elute: recrystallisation by layering light petroleum (30–40 °C) onto a solution of the product in the minimum volume of dichloromethane yielded **1** (77 mg, 66%) (Found: C, 75.55; H, 7.3; N, 5.25. $C_{67}H_{77}F_5N_4O_2$ requires C, 75.73; H, 7.24; N, 5.47%); R_F($CHCl_3$) 0.73; λ_{max}/nm (log ε/dm^3 mol^{-1} cm^{-1}) 410 (5.30), 508 (4.29), 541 (3.70), 575 (3.91), 626 (3.15) and 655 (2.83); ν_{max}(KBr)/cm^{-1} 1759 (C=O); δ_H(500 MHz) −2.34 (2H, br s), 1.15 (12H, m), 1.56 (18H, s), 1.80 (8H, m), 2.22 (8H, m), 2.51 (6H, s), 2.54 (6H, s), 4.03 (8H, t, *J* 7.4), 7.86 (1H, s), 7.96 (2H, s), 8.33 (2H, d, *J* 7.9), 8.59 (2H, d, *J* 8.0) and 10.29 (2H, s); δ_F(235 MHz) −152.52 (2F, d, *J* 20), −158.17 (1F, t, *J* 22.7) and −162.56 (2F, t, *J* 21.5); δ_C(125 MHz) 14.45, 15.35, 23.55, 23.63, 26.73, 31.91, 35.40, 35.73, 97.39, 115.60, 120.18, 121.45, 125.76 (br m), 126.85, 127.75, 129.99, 134.03, 135.51, 137.08, 138.32 (br d, *J* 251), 141.04, 141.60, 141.77 (br d, *J* 252), 141.85, 143.48, 143.92, 144.38, 145.65, 150.06, 150.22 and 163.13; *m/z* (+ve FAB) 1066.0 (M^+).

4-[2,8,12,18-Tetrabutyl-3,7,13,17-tetramethyl-15-(3,5-di-*tert*-butylphenyl)-21*H*,23*H*-porphyrin-5-yl]benzoic acid *n*-propylamide 10

Oxalyl chloride (2.0 cm^3, 16 mmol) was added to a suspension of **8** (200 mg, 2.2 × 10^{-4} mol) in dry dichloromethane (5 cm^3) under nitrogen. It was stirred for 0.5 h and the solvent removed on the vacuum line. The acid chloride formed was not isolated but could be characterised by ^{1}H NMR spectroscopy: δ_H(200 MHz; $CDCl_3$) −0.98 (4H, s), 1.14 (12H, t, *J* 7.0), 1.57 (18H, s), 1.76 (8H, m), 2.17 (8H, m), 2.22 (6H, s), 2.26 (6H, s), 3.66 (8H, t, *J* 7.3), 7.93 (1H, s), 8.12 (2H, s), 8.48 (2H, d, *J* 8.0), 8.66 (2H, d, *J* 8.0) and 10.27 (2H, s). It was redissolved in dry dichloromethane (5 cm^3), neutralised with *p*-dimethylaminopyridine (0.25 g, 2 mmol) and propylamine (0.131 g, 2.2 mmol) was then added in dry dichloromethane (1 cm^3). After stirring for 15 min the product was purified by elution through a short silica plug. Recrystallisation by layering methanol onto a solution of the product in chloroform yielded **10** (140 mg, 67%); R_F($CHCl_3$) 0.27; λ_{max}/nm (log ε/dm^3 mol^{-1} cm^{-1}) 410 (5.32), 508 (4.20), 541 (3.67), 574 (3.85) and 626 (3.30); ν_{max}(KBr)/cm^{-1} 1632 (C=O); δ_H(200 MHz; $CDCl_3$) −2.41 (2H, s), 1.13 (15H, m), 1.50 (9H, s), 1.55 (9H, s), 1.77 (10H, m), 2.16 (8H, br m), 2.45 (12H, s), 3.64 (2H, q, *J* 6.6), 3.98 (8H, t, *J* 7.4), 6.48 (1H, t, *J* 6.7), 7.78 (1H, t, *J* 1.8), 7.90 (2H, d, *J* 1.7), 8.15 (4H, s) and 10.23 (2H, s); *m/z* (+ve FAB) 940.9 (M^+).

4-{2,8,12,18-Tetrabutyl-3,7,13,17-tetramethyl-15-(3,5-di-*tert*-butylphenyl)-5-[4-(*N*-propylcarbamoyl)phenyl]porphyrinato}-zinc(II) 10

A mixture of **10** (60 mg, 6.4 × 10^{-5} mol) and zinc acetate dihydrate (140 mg, 6.4 × 10^{-4} mol) were dissolved in chloroform and heated to reflux for several min. TLC and UV showed the reaction to be complete after 5 min. The product was purified by elution through a short silica plug using chloroform. Recrystallisation from light petroleum (30–40 °C) layered onto a solution of the product in dichloromethane yielded **Zn-10** (60 mg, 94%) (Found: C, 76.4; H, 8.65; N, 7.15. $C_{64}H_{83}N_5OZn$ requires C, 76.58; H, 8.33; N, 6.98%); R_F($CHCl_3$) 0.37; λ_{max}/nm (log ε/dm^3 mol^{-1} cm^{-1}) 412 (5.71), 538 (4.43) and 575 (4.20); ν_{max}(KBr)/cm^{-1} 1641 (C=O); δ_H(500 MHz) 1.15 (15H, m), 1.56 (9H, s), 1.57 (9H, s), 1.78 (6H, m), 1.83 (4H, m), 2.18 (4H, qn, *J* 7.6), 2.21 (4H, qn, *J* 7.6), 2.41 (6H, s), 2.50 (6H, s), 3.61 (2H, m), 3.94 (4H, d, *J* 7.2), 4.02 (4H, t, *J* 7.7), 6.52 (1H, br t), 7.87 (1H, s), 7.99 (2H, s), 8.13 (2H, br d), 8.16 (2H, br d) and 10.20 (2H, s); δ_C(125 MHz) 11.63, 14.21, 14.83, 15.52, 23.07, 23.31, 23.38, 26.37, 26.49, 31.65, 35.15, 35.46, 42.00, 97.66, 117.71,

121.02, 121.38, 125.85, 127.91, 133.49, 134.13, 137.49, 138.65, 142.29, 143.35, 143.56, 146.30, 146.49, 147.15, 147.35, 147.98, 149.70 and 167.43; *m/z* (+ve FAB) 1003.9 (M^+).

Silylation of glass surfaces

Four slides of cleaned glass were immersed in dry toluene (50 cm^3) containing 10% v/v 3-aminopropyltriethoxysilane and 2% v/v diisopropylethylamine in a microscope slide holder at 100 °C for 5 h. The slides were then removed and promptly washed in toluene to prevent adherence of polysilyl particles and then in 1:1 v/v acetone–toluene. The slides were then dried under vacuum. Slides so prepared were used the same day or stored under nitrogen (to prevent surface carbonate formation from atmospheric carbon dioxide).

Glass·H_2-11

Two slides of freshly prepared aminopropylsilylated glass were placed in a test tube containing dry toluene (15 cm^3) and **1** (typically 15 mg, 1.4×10^{-5} mol) and heated to 100 °C for 1 h. The glass was then removed and washed with 10% v/v trifluoroacetic acid in dichloromethane (2×15 cm^3), dichloromethane (15 cm^3), saturated aqueous sodium hydrogen carbonate (15 cm^3), acetone (30 cm^3) and finally dichloromethane (30 cm^3); $\lambda_{max}(CH_2Cl_2)$/nm 417, 513, 542 and 580.

Glass·Zn-11

Zinc acetate dihydrate (150 mg, 6.8×10^{-4} mol) was added to **Glass·H_2-11** (two slides) in chloroform (20 cm^3) and the suspension heated to reflux for 5 min. Incorporation of the metal was verified by running the UV spectrum of the slide in air to ensure that the Q-band at 508 nm, corresponding to the free base porphyrin, was not visible. The glass was then washed with water, acetone and finally with dichloromethane. It was dried *in vacuo* and found to be indefinitely stable in the dark in air; $\lambda_{max}(CH_2Cl_2)$/nm 424, 548 and 578.

UV titrations with amine ligands

Solution titrations of amines with **5** were performed in dry dichloromethane (typically 2.50 cm^3 in cuvette). Amine solutions were made so that the end point was after the addition of *ca*. 200 μl to the porphyrin solution in the cuvette. Absorbance changes about the Soret band were followed by comparing wavelengths in the region where the intensity was increasing with those where it was decreasing.

Titrations involving porphyrin coated glass were essentially the same in practice, with the glass being cut into pieces about 15 × 5 mm and placed in the dichloromethane in the cuvette. For enhanced signal to noise resolution two pieces of glass were typically used in one cell. As the overall signal intensity change is 0.05–0.1 and is critically dependent on the orientation of the slides in the cuvette it is essential to follow the titration by monitoring pairs of wavelengths so as to subtract any fluctuations in the base line absorbance.

All binding curves were fitted using a least-squares curve fitting program[21] for 1:1 binding as there was no evidence that a more sophisticated model should be used.

Acknowledgements

This research was supported by the University of Oxford with generous assistance for D. W. J. M. from Pembroke College, Oxford and British Tar Products Limited. We thank the EPSRC Mass Spectrometry Service in Swansea for FAB mass spectra.

References

1 M. R. Wasielewski, *Chem. Rev.*, 1992, **92**, 435; M. Bixon, J. Fajer, G. Feher, J. H. Freed, D. Gamliel, A. J. Hoff, H. Levanon, K. Möbius, R. Nechushtai, J. R. Norris, A. Scherz, J. L. Sessler and D. Stehlik, *Isr. J. Chem.*, 1992, **32**, 369.
2 (*a*) T. J. Savenije, R. B. M. Koehorst and T. J. Schaafsma, *Chem. Phys. Lett.*, 1995, **244**, 363; (*b*) S.-T. Yang and L. G. Bachas, *Talanta*, 1994, **41**, 963; (*c*) T. L. Blair, J. R. Allen, S. Daunert and L. G. Bachas, *Anal. Chem.*, 1993, **65**, 2155.
3 K. Takahashi, K. Hashimoto, T. Komura and K. Murata, *Chem. Lett.*, 1994, 269.
4 C.-Y. Liu, T. Hasty and A. J. Bard, *J. Electrochem. Soc.*, 1996, **143**, 1914.
5 C. W. Tang, *Appl. Phys. Lett.*, 1986, **48**, 183.
6 (*a*) M. B. Grieve, T. Richardson, H. L. Anderson and D. D. C. Bradley, *Thin Solid Films*, 1996, **285**, 648; (*b*) M. T. Martin and D. Mobius, *Thin Solid Films*, 1996, **285**, 663; (*c*) R. Bonnett, S. Ioannou, A. G. James, C. W. Pitt and M. M. Z. Soe, *J. Mater. Chem.*, 1993, **3**, 793; (*d*) X. Qian, Z. Tai, X. Sun, S. Xiao, H. Wu, Z. Lu and Y. Wei, *Thin Solid Films*, 1996, **285**, 432.
7 T. Akiyama, H. Imahori and Y. Sakata, *Chem. Lett.*, 1994, 1447; T. Akiyama, H. Imahori, A. Ajawakom and Y. Sakata, *Chem. Lett.*, 1996, 907; L.-H. Guo, G. McLendon, H. Razafitrimo and Y. Gao, *J. Mater. Chem.*, 1996, **6**, 369; K. Schimazu, M. Takechi, H. Fujii, M. Suzuki, H. Saiki, T. Yoshimura and K. Uosaki, *Thin Solid Films*, 1996, **273**, 250.
8 (*a*) D. Li, C. T. Buscher and B. I. Swanson, *Chem. Mater.*, 1994, **6**, 803; (*b*) G. A. Schick and Z. Sun, *Thin Solid Films*, 1994, **248**, 86; (*c*) E. Wang and M. E. Meyerhoff, *Anal. Chim. Acta*, 1993, **283**, 673; (*d*) J. Xiao, C. E. Kibbey, D. E. Coutant, G. B. Martin and M. E. Meyerhoff, *J. Liq. Chromatogr. Relat. Technol.*, 1996, **19**, 2901; (*e*) J. Xiao and M. E. Meyerhoff, *J. Chromatogr. A*, 1995, **715**, 19.
9 T. J. Savenije, C. H. M. Marée, F. H. P. M. Habraken, R. B. M. Koehorst and T. J. Schaafsma, *Thin Solid Films*, 1995, **265**, 84; J. Wienke, F. J. Kleima, R. B. M. Koehorst and T. J. Schaafsma, *Thin Solid Films*, 1996, **279**, 87; P. R. Cooke, C. Gilmartin, G. W. Gray and J. R. Lindsay Smith, *J. Chem. Soc., Perkin Trans. 1*, 1995, 1573.
10 (*a*) H. L. Anderson, S. Anderson and J. K. M. Sanders, *J. Chem. Soc., Perkin Trans. 1*, 1995, 2231; (*b*) I. P. Danks, I. O. Sutherland and C. H. Yap, *J. Chem. Soc., Perkin Trans. 1*, 1990, 421.
11 J. P. Mackay, U. Gerhard, D. A. Beauregard, M. S. Westwell, M. S. Searle and D. H. Williams, *J. Am. Chem. Soc.*, 1994, **116**, 4581; P. Adler, S. J. Wood, Y. C. Lee, R. T. Lee, W. A. Petri, Jr. and R. L. Schnaar, *J. Biol. Chem.*, 1995, **270**, 5164.
12 B. L. Iverson, R. E. Thomas, V. Kral and J. L. Sessler, *J. Am. Chem. Soc.*, 1994, **116**, 2663.
13 J. L. Sessler, M. R. Johnson, S. E. Creager, J. C. Fettinger and J. A. Ibers, *J. Am. Chem. Soc.*, 1990, **112**, 9310.
14 R. Wilson and D. J. Schiffrin, *Analyst*, 1995, **120**, 175; H. H. Weetall, *Methods Enzymol.*, 1976, **44**, 134.
15 P. Vandervoort and E. F. Vansant, *J. Liq. Chromatogr. Relat. Technol.*, 1996, **19**, 2723; L. I. Andersson, C. F. Mandenius and K. Mosbach, *Tetrahedron Lett.*, 1988, **29**, 5437.
16 G. S. Marbury, C. Brewer and G. Brewer, *J. Chem. Soc., Dalton Trans.*, 1991, 1377; G. A. McDermott and F. A. Walker, *Inorg. Chim. Acta*, 1984, **91**, 95; D. W. J. McCallien and J. K. M. Sanders, unpublished work.
17 S. Subramanian and M. J. Zaworotko, *Angew. Chem., Int. Ed. Engl.*, 1995, **34**, 2127.
18 F. R. Fronczek, M. L. Ivie and A. W. Maverick, *Acta Crystallogr., Sect. C*, 1990, **46**, 2057.
19 G. Scherowsky and M. Sefkow, *Mol. Cryst. Liq. Cryst.*, 1991, **202**, 207.
20 M. S. Newman and L. F. Lee, *J. Org. Chem.*, 1972, **37**, 4468.
21 W. H. Press, B. P. Flannery, S. A. Teukolsky and W. T. Vetterling, *Numerical Recipes in Pascal*, Cambridge University Press, 1989.

Paper 7/01968H
Received 20*th March* 1997
Accepted 19*th May* 1997